Resonant driving of chaotic orbits

Henry E. Kandrup,* Robert A. Abernathy,† and Brendan O. Bradley‡
Department of Astronomy, University of Florida, Gainesville, Florida 32611
(Received 12 January 1995)

Finite time segments of chaotic orbits in strongly nonintegrable potentials often exhibit complicated power spectra, which, despite being broadband, are dominated by frequencies ω appropriate for "nearby" regular orbits. This implies that even low amplitude periodic driving can trigger complicated resonant couplings, evidencing a sensitive dependence on the driving frequency Ω. Numerical experiments involving individual chaotic orbits indicate that the response to a low amplitude time-periodic perturbation, as measured, e.g., by the maximum excursion in energy arising within a given time interval, can exhibit a sensitive dependence on Ω, with substantial structure even on scales $\delta\Omega < 10^{-4}$ times a typical natural frequency ω. Ensembles of chaotic initial conditions driven with a frequency Ω comparable to the natural frequencies of the unperturbed orbits typically display diffusive behavior: The distribution of energy changes, $N(\delta E(t))$, at any given time t is Gaussian and the rms value of the change in energy $\delta E_{\rm rms} = A(\Omega,E)\alpha t^{1/2}$, where α denotes the driving amplitude. For fixed energy E, the proportionality constant A is independent of the detailed choice of initial conditions, but can exhibit a complicated dependence on Ω. Potential implications for galactic dynamics are discussed.

PACS number(s): 05.90.+m, 51.10.+y, 98.10.+z

I. INTRODUCTION AND MOTIVATION

Recent years have seen a growing interest in the possible role of chaotic (i.e., stochastic) orbits in a number of different astronomical settings, including problems in galactic dynamics [1]. This interest has led many galactic dynamicists to embrace various techniques that have been developed in the nonlinear dynamics community, and that have already found fruitful applications in various other fields of astronomy, including solar system dynamics.

Unfortunately, however, many of these techniques, including the computation of Liapounov exponents, involve asymptotic $t \to \infty$ limits which, in the context of galactic dynamics, are difficult to justify. In terms of their natural timescale, a characteristic crossing time $t_{\rm cr}$, galaxies are relatively young, typically $\sim(100-200)t_{\rm cr}$ in age, so that many aspects of their behavior may be intrinsically transient in character. Thus, in particular, many details that "wash out" on long time scales may be quite important over times as short as $\sim(100-200)t_{\rm cr}$.

This fact implies that individual chaotic orbits can be difficult to characterize on short time scales, especially given the existence of cantori [2] and other partial obstructions, which can partition the stochastic phase space regions into several nearly disjoint pieces. However, it *is* still possible to obtain useful information about problems related to shorter time evolution if one chooses to focus on collections of orbits rather than on the detailed properties of individual trajectories. This recognition has led to the proposal of a theory of transient ensemble dynamics [3,4], which focuses exclusively on the statistical properties of ensembles of stochastic orbits, emphasizing the transient features associated with a short time evolution.

Over the past several decades there has also emerged a growing realization that the standard modeling of galaxies as isolated, time-independent equilibria may be somewhat too naive. Starting with the pioneering simulations of Toomre and Toomre [5], it has been recognized that collisions and other close encounters between galaxies can have a significant influence on the shapes of galaxies, and there is growing observational evidence [6] that many galaxies bear imprints indicating that they have experienced significant interactions with their neighbors. In particular, high resolution photometry has provided evidence that many galaxies, especially those located in rich cluster environments, have shapes more complicated than can be explained by either axisymmetric or plane symmetric triaxial figures observed in projection [7].

This is significant because the simple models that astronomers are wont to consider may be structurally unstable in the sense that even relatively small changes in shape can significantly alter the properties of the orbits entering into a self-consistent equilibrium or near equilibrium. Thus, for example, it has been determined numerically [8] that breaking plane symmetries through the introduction of $l=3$ or 4 harmonic perturbations can greatly increase the overall amount of stochasticity, as probed, e.g., by the Kolmogorov entropy. Similar effects can also arise if some model is perturbed by inserting a large point mass that could mock the gravitational influences of a supermassive black hole [8,9].

*Also at Institute for Fundamental Theory and Department of Physics, University of Florida. Electronic address: kandrup@astro.ufl.edu
†Electronic address: raa@astro.ufl.edu
‡Electronic address: brendan@astro.ufl.edu

Such investigations of the effects of broken spatial symmetries are extremely important. However, if one attributes these broken symmetries to the perturbing influences of an external environment, it would seem natural to allow for the effects of temporal symmetry breaking as well, recognizing that the observed spatial irregularities could signal a bulk gravitational potential that is changing systematically in time. In this connection, it is also important to recognize that even an isolated system can exhibit low amplitude periodic oscillations. There are analytic demonstrations [10] that the collisionless Boltzmann equation does in fact admit solutions corresponding to finite amplitude, systematic oscillations, as well as numerical evidence that such oscillations could arise from an N-body evolution, both in one dimension [11] and, perhaps more controversially, in three [12].

Even if one does not accept the possibility that an isolated galaxy could exhibit systematic periodic oscillations, he or she must recognize that galaxies are inevitably subjected to time-dependent perturbations. However, any such perturbation can be Fourier decomposed into a sum of periodic disturbances, and it is natural to analyze the effects of a single disturbing frequency before studying possible mode-mode couplings associated with multiple periodicities. It would, therefore, seem useful to investigate the short time ($t < 100-200 t_{\rm cr}$) response of chaotic orbits to relatively low amplitude periodic driving, both at the level of individual orbits and in terms of the behavior of ensembles of orbits. Such is the purpose of this paper.

Most of the calculations described herein involved perturbations of one simple two degree of freedom system, characterized by a time-independent Hamiltonian

$$H=\tfrac{1}{2}(p_x^2+p_y^2)-\frac{1}{(c^2+x^2+y^2)^{1/2}} -\frac{m}{(c^2+x^2+a^2y^2)^{1/2}}\ , \tag{1}$$

with $c=1.0$, $m=0.3$, and $a^2=0.1$. For typical energies corresponding to bound orbits, a characteristic crossing time in this potential is, in absolute units, of order $t_{\rm cr}\sim 10-20$, so that the age of the Universe, t_H, corresponds to a time $t\sim 2000$. The perturbations involved the introduction of periodic oscillations in the core radius c and the asymmetry parameter m, assuming

$$c(t)=c(1+\alpha_c\cos\Omega t) \text{ and } m(t)=m(1+\alpha_m\cos\Omega t)\ . \tag{2}$$

For a broad range of energies, this Hamiltonian admits both regular and stochastic orbits. Most, if not all, the regular orbits are either loops or boxes. Many of the stochastic orbits are unconfined, moving unimpeded throughout most of the stochastic sea. However, there also exists a nontrivial measure of confined stochastic orbits which, because of the effects of cantori, are trapped on short time scales near the regular islands. Typical examples of loop, box, unconfined stochastic, and confined stochastic orbits are exhibited in Figs. 1(a)–1(d).

The basic results derived in this paper, both qualitative and semiquantitative, are independent of whether c or m is perturbed, which suggests that the detailed form of the perturbing influence is relatively unimportant. Less exhaustive investigations indicate that similar results are also obtained for other nonintegrable potentials admitting large measures of both regular and chaotic orbits, e.g., the so-called D-4 potential [13]. There is, therefore, reason to anticipate that the results reported herein are relatively generic.

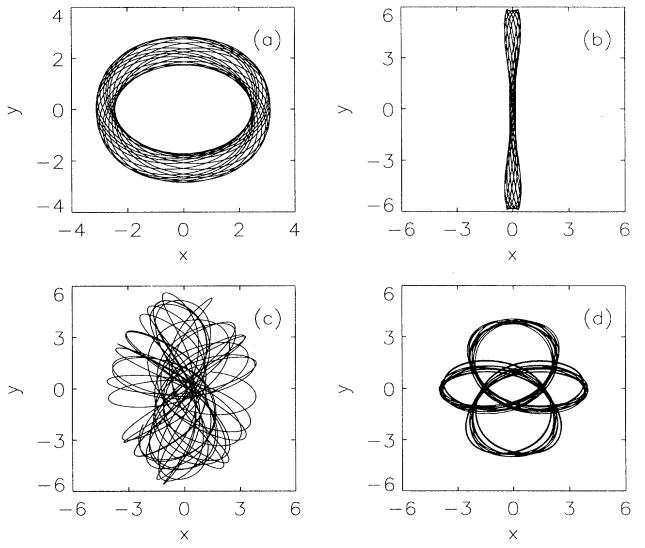

FIG. 1. Four orbits computed for the Hamiltonian (1) with energy $E=-0.3$. (a) A typical loop orbit. (b) A typical box orbit. (c) A typical unconfined stochastic orbit. (d) A typical confined stochastic orbit.

One might naively expect that, because chaotic orbits are manifestly irregular, a simple periodic driving will not trigger a resonant response. This, however, is false. By applying well known spectral techniques [14] to stochastic orbits, one finds [15,16] that, despite exhibiting a power spectrum that is relatively broadband, these orbits are typically dominated by frequencies at or near a few fundamental values. The obvious point, then, is that couplings to these special frequencies can, in fact, trigger a substantial resonant response.

The principal conclusion of the computations reported herein is that, as for the case of regular orbits, the effects of a modest amplitude periodic driving are intrinsically resonant in nature, albeit exhibiting a more complicated response indicative of the existence of a variety of unperturbed frequencies. This complexity implies that, once again, characterizing individual orbits is quite hard. If, however, one focuses on an ensemble of stochastic orbits, e.g., a sampling of an unperturbed invariant [17] or near-invariant [3] measure of energy E_0, one is led to a comparatively simple statistical characterization. In terms of its effects on the bulk properties of the ensemble, periodic driving serves simply to trigger a diffusion process: At any given instant of time, the distribution of changes in energy $N(\delta E(t))$, is Gaussian, with a dispersion that grows as $t^{1/2}$ and that scales linearly in the amplitude of the perturbing influence.

Section II of this paper recalls the qualitative features

of Fourier spectra generated from stochastic orbits, and then contrasts in general terms the effects of periodic driving on regular versus stochastic orbits. Section III turns to a systematic investigation of how, for an individual stochastic orbit, the response to modest periodic driving varies as a function of driving frequency, illustrating in particular that the response can exhibit substantial structure even on very small scales. Section IV shows how this complicated response observed for individual orbits leads at the level of ensembles to a simple diffusive behavior. Section V concludes with some speculations on potential astronomical implications.

II. SPECTRAL ANALYSIS OF STOCHASTIC ORBITS

Suppose, for specificity, that one is given configuration space coordinates $x(t_j)$ and $y(t_j)$, generated for an orbit in some two-dimensional system at j instants of time, each separated by the same fixed interval δt. It is then natural to define a discrete Fourier transform

$$x(\omega_k)=\sum_{j=1}^{N} x(t_j)\exp(-i\omega_k t_j)\ , \tag{3}$$

and the corresponding $y(\omega_k)$, for a set of frequencies $\{\omega_k\}$ with $k \le j$. Because $x(t_j)$ and $y(t_j)$ are, by construction, real numbers, one knows that $x(\omega_k) = x^{\dagger}(-\omega_k)$, where the dagger denotes complex conjugation, so that it is sufficient to consider positive frequencies ω_k. The real and imaginary parts of $x(\omega_k)$ and $y(\omega_k)$ can be viewed separately as being generated by cosine and sine series, and the total power at frequency ω_k is encoded in the magnitudes $|x(\omega_k)|$ and $|y(\omega_k)|$.

For an integrable system, where the orbits are multiply periodic, the true Fourier transforms $|x(\omega)|$ and $|y(\omega)|$ generated from an analytic representation of some orbit will only be nonvanishing for a set of discrete frequencies. However, given the finite resolution associated with the sampling interval δt and the finite total sampling time $(j-1)\delta t$, the computed spectra for a numerical realization of the orbit will, even neglecting roundoff and/or truncation errors, be "fuzzed out" somewhat, although the power will be sharply concentrated near well defined maxima at discrete frequencies.

This behavior is qualitatively identical to that which is observed for regular orbits generated in a nonintegrable potential [14]. If, instead, one considers an orbit in a nonintegrable potential that is chaotic, rather than regular, the computed spectrum can be significantly more complicated. For the case of a confined stochastic orbit, trapped temporarily near an island because of cantori, the form of the spectrum may be nearly indistinguishable from that observed for a regular orbit [16]. However, for the case of an unconfined stochastic orbit, not trapped by cantori and hence free to travel unimpeded throughout most of the stochastic sea, the form of the spectrum is substantially more irregular.

If, for an unconfined stochastic orbit, one focuses on some finite time interval $t_H \sim 100 t_{\rm cr}$ and computes a discrete Fourier transform, he or she will often find that the spectrum is comprised of at least three different components, indicating that, in a real sense, the stochastic orbit contains "pieces" of several different types of regular orbits. Specifically, one typically observes (1) a low level broadband continuum, (2) peaks at a set of frequencies appropriate for one regular orbit, e.g., a box, and (3) peaks at another set of frequencies appropriate for at least one other regular orbit, e.g., a loop. Indeed, the relative power in these different components provides a concrete diagnostic in terms of which to quantify the sense in which some stochastic orbit is almost a box, almost a loop, or a more significant admixture of more than one orbit type [16]. The fact that a stochastic orbit can contain within it "hints" of several different regular orbits is readily understood in terms of the onset of chaos through resonance overlap. This general behavior is exhibited in Figs. 2 and 3, which, respectively, exhibit the Fourier transformed $|x(\omega)|$ and $|y(\omega)|$ for two regular orbits—

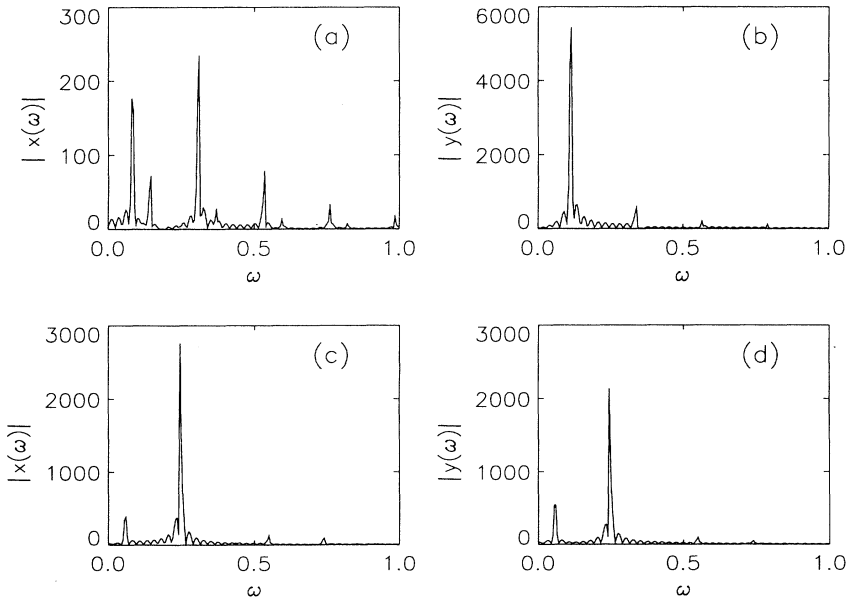

FIG. 2. (a) The power $|x(\omega)|$ associated with a regular box orbit with energy $E=-0.3$, computed in the potential (1). (b) The corresponding $|y(\omega)|$. (c) The power $|x(\omega)|$ associated with a regular tube orbit with energy $E=-0.3$, again computed in the potential (1). (d) The corresponding $|y(\omega)|$.

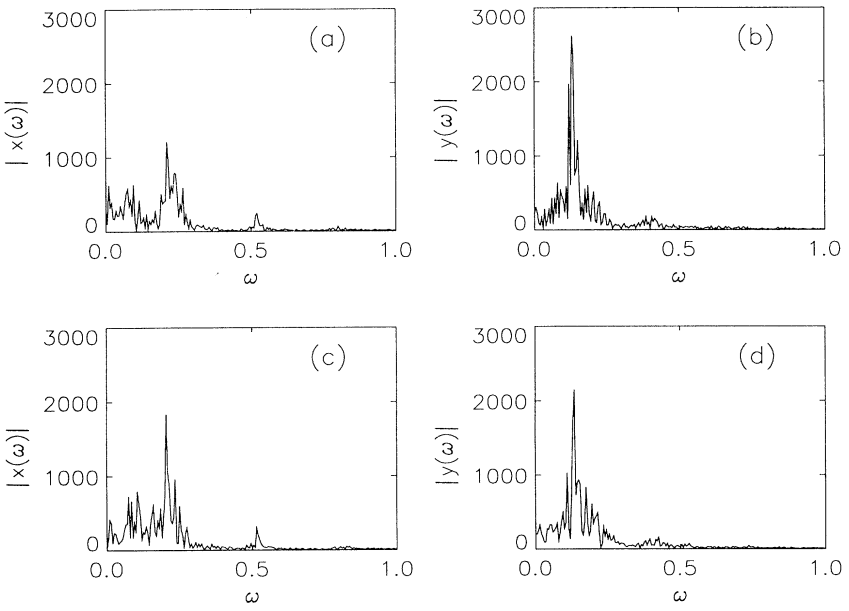

FIG. 3. (a) The power $|x(\omega)|$ associated with one chaotic orbit with energy $E=-0.3$, computed in the potential (1). (b) The corresponding $|y(\omega)|$. (c) The power $|x(\omega)|$ associated with a different chaotic orbit with energy $E=-0.3$, again computed in the potential (1). (d) The corresponding $|y(\omega)|$.

one loop and one box—and two stochastic orbits, each computed in the potential (1) for initial conditions with $E=-0.3$.

It is well known and easily understood that a regular orbit in a nonintegrable time-independent potential will manifest a strong resonant coupling to any periodic driving if the driving frequency Ω is approximately commensurate with one of the natural frequencies associated with the unperturbed orbit. The fact that chaotic orbits can also have spectra characterized by relatively sharp maxima would suggest by analogy that they, too, will be susceptible to resonant coupling. However, because the unperturbed spectra are more complex, one might anticipate that the nature of this coupling will be substantially more complicated: The fact that there are more peaks would suggest that there should be more driving frequencies capable of triggering a resonance, and the broader band character of the overall spectrum might be expected to translate into a complicated pattern of resonances that manifests structure even on very small scales. As will be detailed below, this is, in fact, the case.

One obvious way in which to characterize the response of an orbit to the periodic driving is to compute the change in energy δE for the orbit as a function of time t, and then analyze the amplitude and overall functional form of $\delta E(t)$. One discovers thereby that, for both regular and chaotic orbits, in order to trigger a substantial resonant coupling one must ensure that the driving frequency Ω be in a range comparable to the natural frequencies ω associated with the unperturbed orbit. Thus, e.g., for bound orbits in the model potential (1), the natural frequencies typically reside in the range $\omega\sim 0.05-1.0$, and to obtain a substantial resonant response one requires a driving frequency $\Omega\sim 0.05-5.0$. If Ω is too high, couplings to harmonics of the natural frequencies will not be strong enough to trigger much of a response.

If a regular orbit is driven at a frequency Ω that is in near resonance with one of its natural frequencies, one typically observes a substantial systematic response whereby a plot of $\delta E(t)$ exhibits slow, regular oscillations with a period that can be extremely long. Thus, e.g., for both box orbits and loop orbits in the potential (1) with energy $E\sim -0.3$, one finds that the natural frequencies exhibiting the largest power are typically of order $\omega\sim 0.1-0.4$ and that the driving frequencies that trigger the largest response are of order $\Omega\sim 0.2-5.0$, but that the observed periodicities can be as long as $\tau\sim 800$ or more. For fixed driving frequency Ω, the overall size of the response, as measured by the amplitude $\delta E_{\max}/|E_0|$ of the periodic oscillation, varies nearly linearly with the amplitude $\alpha_{c,m}$ of the driving, at least for $\alpha_{c,m}<10^{-2}$ or so, and is itself comparable in magnitude to $\alpha_{c,m}$. The periodicity of $\delta E(t)$ and the overall shape of the curve are approximately independent of $\alpha_{c,m}$. Away from resonance, the amplitude of the response is smaller overall, but still scales with $\alpha_{c,m}$ in a near-linear fashion.

Away from a resonance, the amplitude decreases significantly, by an order of magnitude or more, even if the driving frequency remains in the "natural" range $\Omega\sim 0.05-5.0$. Moreover, the simple long term periodicity is lost, although it usually remains possible to identify a more complicated multiperiodic pattern. If one estimates a "characteristic" periodicity τ by identifying the total number of sharply defined maxima arising within a fixed time interval, say, $t=1000$, he or she finds that there exists a strong inverse correlation between the amplitude of the response and the characteristic periodicity. In particular, a plot of τ as a function of the maximum response $\delta E_{\max}$ arising within a period $t=1000$ is relatively well fit by a simple scaling $\tau\propto \delta E_{\max}^{p}$, with $p\sim -1$.

This general behavior is illustrated in Fig. 4, which exhibits the time-dependent change in energy, $\delta E(t)$, for several different realizations of the same initial condition, allowing for a perturbation $\alpha_m=10^{-3}$ and driving frequencies $0.50\le\Omega\le 1.30$. This particular initial condition

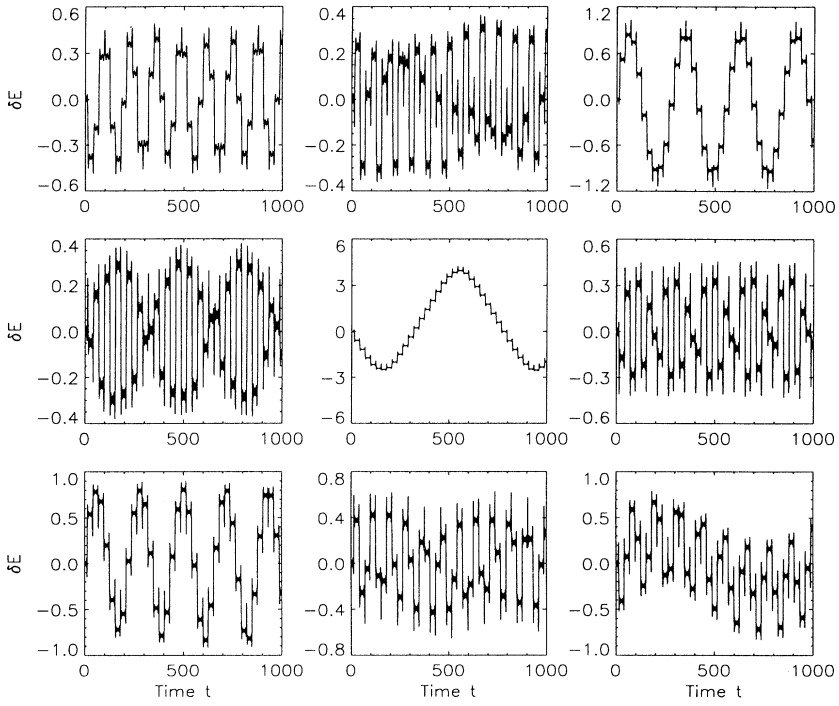

FIG. 4. The rescaled energy response, $10^3\delta E(t)$, computed for one initial condition, corresponding to an unperturbed box orbit with $E=-0.3$, allowing for a perturbation in m of amplitude $\alpha_m=10^{-3}$ and variable driving frequencies between $\Omega=0.50$ and $\Omega=1.30$, increasing from left to right and top to bottom, by uniform increments of $\Delta\Omega=0.10$.

corresponds to the box orbit exhibited in the first two panels of Fig. 2.

When subjected to periodic driving, stochastic orbits do not exhibit a comparable pattern of coherent oscillations. Moreover, the shape of the curve $\delta E(t)$ is no longer independent of the amplitude $\alpha_{c,m}$. However, the response *is* similar to that exhibited by regular orbits in that (1) the overall amplitude still scales roughly linearly in $\alpha_{c,m}$ and (2) relatively small changes in Ω can alter the amplitude of the response by an order of magnitude or more.

For a variety of different initial conditions, the largest observed growth of $|\delta E|/|E_0|$ within a time $t=1000$ was to value $\sim 10-50\alpha_{c,m}$. This robust response entailed a roughly linear growth in $|\delta E|$, probably associated with an evolution dominated by a single resonance. On longer

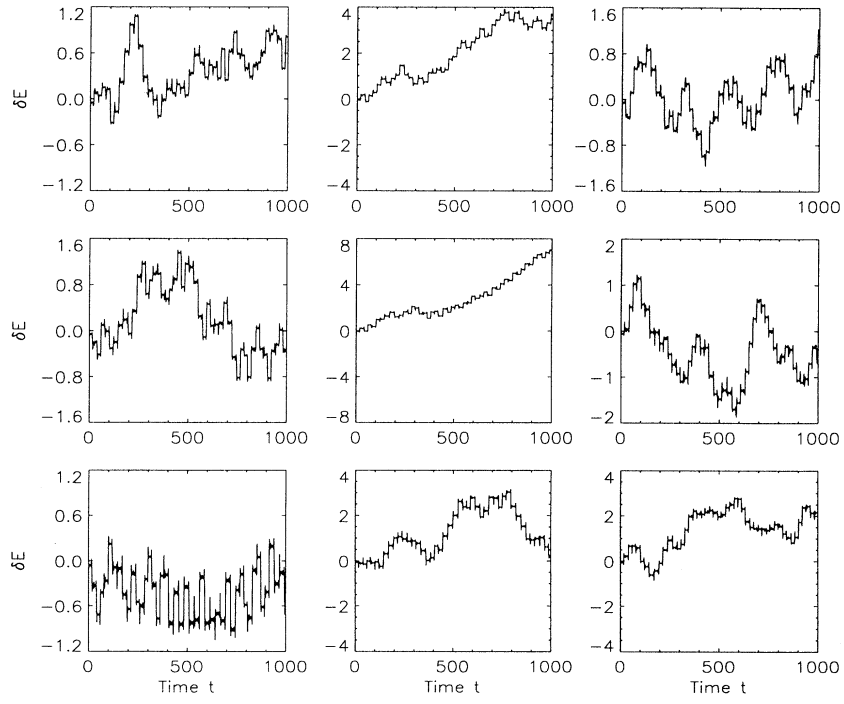

FIG. 5. The same as Fig. 3, except for an unconfined stochastic orbit with $E=-0.3$.

times $t>1000$, the growth eventually decelerates, presumably in response to the fact that changes in the orbital energy have moved the orbit away from resonance. This behavior is, however, atypical. More commonly observed is a substantially weaker response, manifestly irregular in form, which would suggest that the orbit is executing an approximate random walk in energy space.

This behavior is illustrated in Fig. 5, which exhibits the time-dependent change in energy, $\delta E(t)$, for several different realizations of the same initial condition, again allowing for a perturbation $\alpha_m=10^{-3}$ and driving frequencies $0.50\leq\Omega\leq 1.30$. This particular initial condition corresponds to the chaotic orbit exhibited in the first two panels of Fig. 3. A comparison of Figs. 4 and 5 reveals that, overall, the chaotic orbit experiences larger changes in energy than does the regular orbit. This is a general feature, observed for most initial conditions, the implications of which will be considered in Sec. V.

III. RESONANT DRIVING OF INDIVIDUAL ORBITS

Unless otherwise noted, each of the series of numerical experiments described in this section involved a computation of orbits in a perturbed version of the potential (1), with multiple integrations being effected for a number of different initial conditions, corresponding to both regular and chaotic orbits. The perturbations all involved subjecting m or c to periodic oscillations with the same amplitude $\alpha_{c,m}=10^{-3}$, since, as discussed already, the response to the perturbation scales approximately linearly in the amplitude. For each initial condition, with α_c or α_m nonzero, Ω was varied between 0.00 and 5.00 in small increments $\delta\Omega=0.025$, resulting in 201 different integrations. Each integration proceeded for a total time $t=1000$, with orbital data being recorded at fixed $\delta t=0.5$ intervals. The output from each integration was analyzed to extract several different quantities, including the maximum energy excursion $\delta E_{\max}$ and the mean energy excursion

$$\delta E_{\text{mean}}=\frac{1}{j}\sum_{j=0}^{2000}|E(t_j)-E(0)|\ , \tag{4}$$

arising over the fixed interval, as well as several other diagnostics that quantify the strength of the resonant coupling.

If, for a regular orbit, $\delta E_{\max}$ is plotted as a function of Ω, one observes a simple, highly regular response, with sharply defined peak frequencies Ω_i. Moreover, one observes that the locations of these driving frequencies correlate directly with the values of the natural frequencies associated with the unperturbed regular orbits. Thus, in particular, the values of the peak frequencies Ω_i are seemingly independent of whether the core radius or the asymmetry parameter is oscillating, although the amplitudes of the maxima do depend on whether it is α_c or α_m that is nonvanishing.

This behavior is illustrated in Figs. 6(a)–6(d), which summarize data obtained for two different regular initial conditions with $E=-0.3$, (a) and (c) corresponding to the box orbit exhibited in Fig. 2 and (b) and (d) to the loop of Fig. 2. Figures 6(a) and 6(b) show the maximum energy excursion $\delta E_{\max}$ obtained when c oscillates, and Figs. 6(c) and 6(d) show the corresponding data generated by varying m. It should be obvious from this figure that, overall, the peak frequencies are the same when c and m oscillate. However, the intensities of the peaks, both in absolute units and in relative strengths, are different when c and m are allowed to vary, although these differences are usually relatively small, i.e., typically less than a factor of two. Particularly obvious is the fact that the low level continuum arising when c and m oscillate is virtually identical.

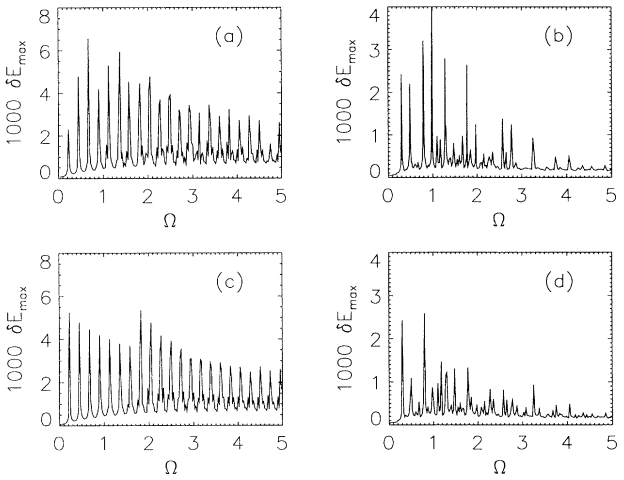

FIG. 6. (a) The rescaled maximum energy response, $10^3\delta E_{\max}$, computed as a function of driving frequency Ω, for a box orbit with unperturbed energy $E=-0.3$, subjected to a pulsation in c of amplitude $\alpha_c=10^{-3}$. (b) The same quantity computed for a loop orbit with unperturbed energy $E=-0.3$ for an identical perturbation $\alpha_c=10^{-3}$. (c) The same quantity computed for the box orbit of (a), now allowing for a pulsation in m with the same amplitude $\alpha_m=10^{-3}$. (d) The same quantity computed for the loop orbit of (b), allowing for a pulsation in m of amplitude $\alpha_m=10^{-3}$.

Less obvious but also true is the fact that the patterns of resonances in Figs. 6 are directly related to the natural frequencies of the unperturbed orbits. Thus, e.g., for the box orbit in Figs. 6(a) and 6(c), the natural unperturbed frequencies for $|x(\omega)|$ and $|y(\omega)|$ occur at values $\omega_1\approx 0.0825$ and $\omega_2\approx 0.060$, with the dominant peak and successive harmonics for $|y(\omega)|$ occuring at frequencies $(2n+1)\omega_c$, where $\omega_c=\omega_1+0.5\omega_2\approx 0.1125$. However, $\delta E_{\max}$ exhibits successive maxima at frequencies $2n\omega_c\approx 0.225n$. For the loop orbit of Figs. 6(b) and 6(d), the natural unperturbed frequencies are $\omega_1\approx 0.060$ and $\omega_2\approx 0.190$, but the successive maxima of $\delta E_{\max}$ are given as harmonics of the fundamental frequencies $\Omega_1=\omega_2+2\omega_1$ and $\Omega_2=\omega_2$. Similar patterns are observed for other regular orbits.

Figure 6 exhibit the maximum response $\delta E_{\max}$. However, analogous results are also obtained if one computes different measures of the resonant response. Thus, e.g., a plot of δE_{mean} looks almost identical to a plot of $\delta E_{\max}$ except for the fact that the amplitude is smaller by a fac-

tor of roughly 2.

If $\delta E_{\max}$ is plotted instead for a chaotic orbit, one still obtains a strongly resonant response. However, the overall pattern is substantially more complex and, as would be expected, cannot be explained completely in terms of two or three fundamental frequencies. However, despite these additional complications, the response of a chaotic orbit resembles that of a regular orbit in that the peak frequencies typically occur at $\Omega \sim 1$, and that the response is generally much weaker for $\Omega > 5$ or so. Moreover, the peak frequencies again appear to be relatively insensitive to how the orbit has been perturbed, in that the responses to oscillations in c and m are comparable in magnitude.

This general behavior is exhibited in Figs. 8(a)–8(d), which summarize data obtained for the two chaotic orbits with $E = -0.3$ exhibited in Fig. 3. As in Fig. 6, the first two panels exhibit the maximum change in energy, $\delta E_{\max}(\Omega)$, obtained by pulsing c and the second two by pulsing m. The overall form of the response here is clearly much more complex than in Figs. 6, but the coupling is still unambiguously resonant in the sense that a strong response arises only for specific frequencies. The observed patterns when c and m are varied are again relatively similar, but one observes conspicuous differences in that frequencies Ω which are especially effective when m oscillates can be quite ineffective when it is c that varies (and visa versa). For the case of chaotic orbits, it is again true that δE_{mean} and other similar quantities exhibit the same resonant response as does $\delta E_{\max}$. One also observes that, as for the case of regular orbits, the form of the continuum contribution to $\delta E_{\max}$ is very similar for orbits in which c and m are varied, much more similar in fact than the form of the resonant spikes.

The obvious feature arising in the resonant driving of chaotic orbits is that the response, as measured by $\delta E_{\max}$ or any similar quantity, is extremely complex. This complexity arises presumably as a result of the fact that there is now a much larger number of natural frequencies to which the driving can couple. However, this, in turn, might suggest that a curve of $\delta E_{\max}(\Omega)$ should exhibit a good deal of structure, even on very short scales: Because the distribution of "fundamental frequencies" is very complicated, with the peak frequencies having a relatively large bandwidth, there should exist a large number of different driving frequencies Ω that could resonate with various combinations of natural frequencies.

The fact that structure exists even down to very small scales is manifest explicitly in Fig. 8, which presents a sequence of plots of $\delta E_{\max}(\Omega)$, generated over successively smaller frequency intervals $\Delta\Omega$. All the data in this figure were generated from the initial condition exhibited in Fig. 7(c), again oscillating m with amplitude $\alpha_m = 10^{-3}$. Figure 7(c) sampled 201 points over a frequency range $\Delta\Omega = 5.0$. The four panels in Fig. 7 represent 201 orbit samplings of smaller regions of, respectively, total size $\Delta\Omega = 5.0\times10^{-1}$, 5.0×10^{-2}, 5.0×10^{-3}, and 5.0×10^{-4}.

Figure 8 illustrates the fact that the overall response to the driving exhibits structure even down to very small scales, with $\delta E_{\max}$ changing by a factor of 2 or more overall frequency intervals $< (1-2)\times10^{-5}$. However, there *does* seem to be a clear visual sense in which the plots become more regular as $\Delta\Omega$ is decreased. It should also be noted that, although the response is usually a very sensitive function of Ω, there are certain frequency ranges, e.g., frequencies $\Omega \approx 1.284$ in Fig. 7(c), where the response is much smoother overall.

These latter two facts would suggest that, despite the existence of considerable structure even on very small scales, the dependence on Ω is not completely self-similar. However, even if this dependence is not self-similar, one might expect that, were one to consider statistical properties associated with an ensemble of initial conditions, he or she would observe a seemingly random behavior that is intrinsically diffusive in character.

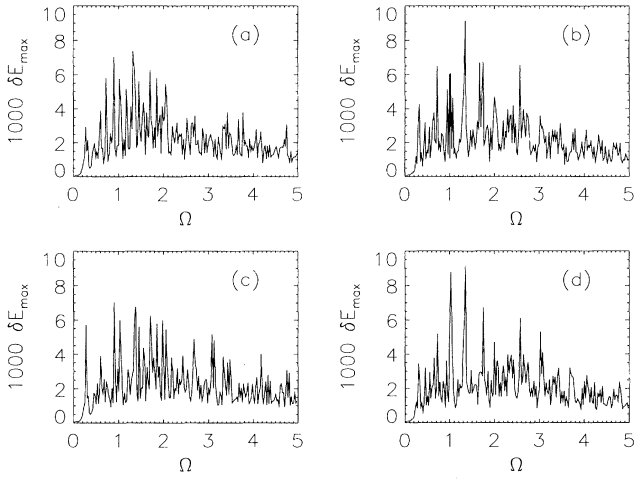

FIG. 7. (a) The rescaled maximum energy response $10^3\delta E_{\max}$ computed as a function of driving frequency Ω, for one chaotic orbit with unperturbed energy $E = -0.3$, subjected to a pulsation in c of amplitude $\alpha_c = 10^{-3}$. (b) The same quantity computed for another with unperturbed energy $E = -0.3$, for an identical perturbation $\alpha_c = 10^{-3}$. (c) and (d) The same quantities computed for the orbits of (a) and (b), now pulsing m with amplitude $\alpha_m = 10^{-3}$.

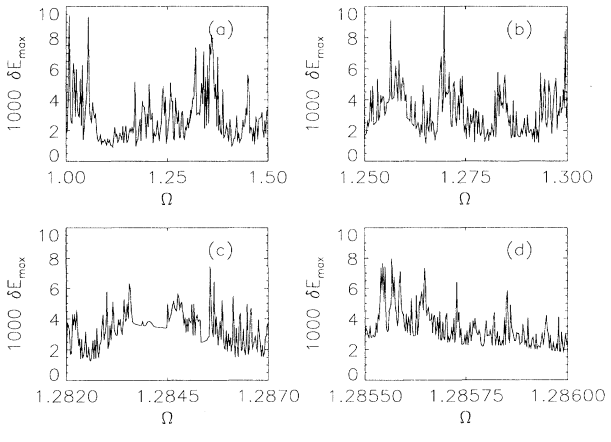

FIG. 8. (a)–(d) An enlargement of Fig. 6(c), focusing on frequency ranges $\Delta\Omega = 5\times10^{-1}$, 5×10^{-2}, 5×10^{-3}, and 5×10^{-4}.

IV. RESONANT DRIVING OF ORBIT ENSEMBLES

The computations summarized in the preceding sections indicate that if an individual chaotic orbit is pulsed with a randomly chosen frequency in the range $0.05 \leq \Omega \leq 5.0$, one will typically observe a substantial, but not huge, response, whereby $\delta E(t)$ exhibits an apparent random walk in energy space. Moreover, if the same experiment are performed for a number of different chaotic orbits, the responses will be similar in bulk but different in the details. In particular, the exact short time form of the resonant pattern is not the same for different orbits, even if all of them are unconfined stochastic orbits with the same unperturbed energy E_0.

This suggests a simple prediction as to what might be seen if one were to select an ensemble of initial conditions, evolve these initial conditions into the future, pulsing either c or m, and then analyze the orbital data to extract such statistical properties as the distribution of energy shifts, $N(\delta E(t))$. Suppose that each orbit in the ensemble is, in fact, executing a random walk in energy space. One would then expect (1) that the distribution $N(\delta E(t))$ at any given instant should be approximately Gaussian, (2) that the mean of the distribution should vanish, and (3) that the dispersion of the distribution should grow as $t^{1/2}$. The observation from Secs. II and III that, for individual orbits, the amplitude of the response scales roughly linearly in $\alpha_{c,m}$ then suggests further that the dispersion of the distribution should vary linearly with $\alpha_{c,m}$.

To test these predictions, a number a different experiments were performed. Each involved an ensemble of 400 different initial conditions, corresponding to orbits with a specified unperturbed energy E_0. Most of the experiments involved ensembles of unconfined stochastic orbits, but others were performed for ensembles of confined and regular orbits. Most of the ensembles were constructed from a sampling of a small phase space region, setting $x=0$, uniformly sampling a small portion of the $\{y,p_y\}$ plane, and then determining a positive $p_x = p_x(y,p_y,E_0)$. However, other experiments were performed for initial conditions generated as a sampling of the near-invariant measure associated with a collection of unconfined stochastic orbits.

In each case, the initial conditions were evolved for a time $t=5000$, allowing for a variable c or m, orbital data being recorded at fixed time intervals. The output was then combined to extract the distribution $N(\delta E(t))$, as well as the first and second moments. The amplitude of the pulsing was varied in the range $10^{-6} \leq \alpha_{c,m} \leq 10^{-2}$, and the driving frequency was varied in the range $0.5 \leq \Omega \leq 100.0$.

As for the case of individual orbits, it was found that, overall, the largest responses arise for $\Omega \sim 1$, independent of orbit class, i.e., for regular and confined orbits as well as unconfined chaotic orbits. For the case of regular and confined chaotic orbits, the observed statistical behavior was often quite complicated. However, for the case of unconfined chaotic orbits with $\Omega \sim 1$, the predicted diffusive behavior was, in fact, usually observed, at least for times $t < 2000$ or so.

At very early times $\delta E_{\rm rms}$, the root mean square (rms) energy for ensemble, can exhibit a complicated transient behavior but, within a time $t \sim 100$, one sees unambiguous indications of a regular $t^{1/2}$ dependence. If, for the time interval $0 \leq t \leq 2000$, one seeks a best fit exponent for a relation $\delta E_{\rm rms} \propto t^p$, the experiments with variable c yield $p_c = 0.53 \pm 0.04$, while those with variable m yield $p_m = 0.57 \pm 0.02$. The best fit overall is $p = 0.54 \pm 0.03$. If one excludes the very early time behavior, the best fit value of p decreases to a value even closer to 0.5.

One also observes that, independent of the amplitude of the perturbing influence (at least for $\alpha_{c,m} < 10^{-2}$ or so) and of how the system is perturbed (i.e., whether it is c or m that is being varied), the distribution $N(\delta E(t))$ is approximately Gaussian in form, with a mean energy $\bar{E}$ satisfying $|\bar{E} - E_0| \ll \delta E_{\rm rms}$. Moreover, one finds that the amplitude of the response does indeed scale linearly in $\alpha_{c,m}$. Thus, in particular, if the same initial conditions are driven in the same quantity with variable amplitude α_c or α_m, and the output is fit to a linear relation $\delta E_{\rm rms}^2 = A^2 \alpha_{c,m}^2 t$, one finds that the best fit values of A for different amplitudes typically agree to better than 5%.

Another significant point is that, in general, $N(\delta E(t))$ and its moments appear to be independent of initial conditions, provided that one considers different ensembles of unconfined stochastic orbits with the same unperturbed energy. Thus, in particular, different ensembles will, when perturbed identically, exhibit the same $\delta E_{\rm rms}(t)$ to within 2–4 %. However, the response does depend on whether it is c or m that oscillates. Just as for the case of individual orbits, the response of an ensemble when varying c and m can differ by close to a factor of 2.

This general behavior is illustrated in Figs. 9 and 10. Figures 9(a) and 9(b) exhibit $\delta E_{\rm rms}(t)$ for the same set of initial conditions, corresponding to 400 unconfined sto-

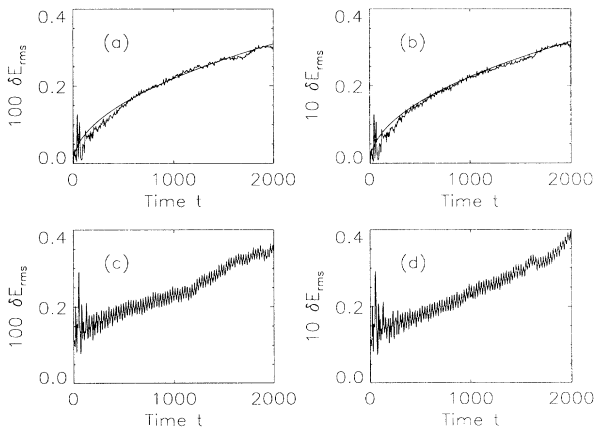

FIG. 9. (a) The rms change in energy $\delta E_{\rm rms}(t)$ for one ensemble of 400 unconfined stochastic orbits with $E=-0.5$, c being pulsed with frequency $\Omega=1.0$ and $\alpha_c=10^{-4}$. (b) The same quantity for the same ensemble, with m pulsed with $\Omega=1.0$ and $\alpha_c=10^{-3}$. (c) The same quantity for another ensemble of unconfined orbits with $E=-0.5$, again with m pulsed with $\Omega=1.0$ and $\alpha_c=10^{-4}$. (d) The same quantity for the same ensemble, with m pulsed with $\Omega=1.0$ and $\alpha_c=10^{-3}$.

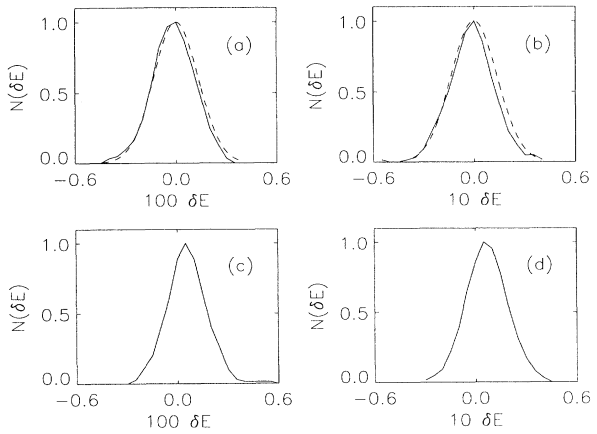

FIG. 10. (a) The distribution of energy shifts, $N(\delta E(t))$, at time $t=1600$, for the same data exhibited in Fig. 9(a). (b) $N(\delta E(t))$ at time $t=1600$ for the data exhibited in Fig. 9(b). (c) $N(\delta E(t))$ at time $t=1600$ for the data exhibited in Fig. 9(c). (d) $N(\delta E(t))$ at time $t=1600$ for the data exhibited in Fig. 9(d).

chastic orbits of energy $E_0=-0.5$, oscillating with frequency $\Omega=1.0$. The first panel exhibits the response to oscillating c with amplitude $\alpha_c=10^{-4}$ and the second to oscillating c with amplitudes $\alpha_c=10^{-3}$. It should be clear that, modulo the scaling in α_c, the responses are essentially identical. The smooth curve in each panel exhibits the best fit to a $t^{1/2}$ relation. Figures 10(a) and 10(b) exhibit the distributions from which the $\delta E_{\rm rms}$ of Figs. 9(a) and 9(b) were computed, evaluated at one representative time, namely $t=1600$. In these panels, the dashed curves represent Gaussian distributions appropriate for the value of $\delta E_{\rm rms}$ exhibited in Figs. 9(a) and 9(b), assuming a zero mean. The fit is again quite good.

The preceding refers to generic behavior. However, it is also possible to find "special" localized ensembles, even for the case of unconfined stochastic orbits, which are dominated early on by a single resonance and, consequently, exhibit a rather different response in which $\delta E_{\rm rms}$ does not exhibit a $t^{1/2}$ dependence.

Examples of this anomalous behavior are shown in Figs. 9(c) and 9(d). These panels both exhibit $\delta E_{\rm rms}(t)$ for the same ensemble of 400 initial conditions with $E_0=-0.5$, with c oscillating with a driving frequency $\Omega=1.0$. The first panel corresponds to an amplitude $\alpha_c=10^{-4}$ and the second to $\alpha_c=10^{-3}$. It is evident that the response is still proportional to α_c, but that the evolution of $\delta E_{\rm rms}$ is no longer given by a simple $t^{1/2}$ growth law. Rather, one observes a rapid jump in $\delta E_{\rm rms}$, followed by a slower subsequent evolution during which the amplitude of $\delta E_{\rm rms}$ attains values comparable to those arising in Figs. 9(a) and 9(b). It should also be observed that, in this case, $\delta E_{\rm rms}(t)$ shows considerably more short scale structure, consistent with the existence of coherent, low amplitude oscillations. It is also significant that, despite these differences, the distributions $N(\delta E(t))$ arising for this ensemble are still reasonably well fit by a Gaussian, albeit with a nonzero mean. This is illustrated

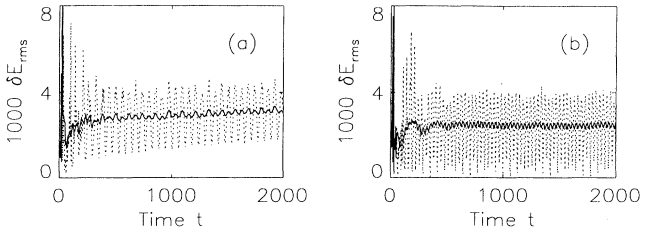

FIG. 11. (a) The rms change in energy $\delta E_{\rm rms}(t)$ for the ensemble of 400 unconfined stochastic orbits with $E=-0.5$ exhibited in Figs. 9(c) and 9(d), with c being pulsed at amplitude $\alpha_c=10^{-3}$ with frequency $\Omega=10.0$. (b) The same as Fig. 11(a), except with $\Omega=100.0$.

in Figs. 10(c) and 10(d), which again exhibit these distributions at time $t=1600$.

Even for those "normal" ensembles exhibiting short time diffusive behavior, deviations can be observed at later times $t>3000-4000$, reflecting two different effects: (1) When analyzing the statistics of a 400 orbit ensemble, one finds that contributions from a relatively small number of orbits exhibiting a systematic linear growth in $\delta E_{\rm rms}$ can eventually outweigh contributions arising from the slower $t^{1/2}$ growth exhibited by a large majority of the orbits; (2) it is also possible that, as time evolves, different stochastic orbits originally exhibiting a random walk can become trapped in a resonance and begin to exhibit a more rapid, linear evolution.

The systematic growth of $\delta E_{\rm rms}$ manifest in Fig. 9 only results because of resonant couplings that are operative at frequencies $\Omega\sim 1$ and, consequently, disappears for much higher or lower frequencies. This is, e.g., illustrated in Figs. 11(a) and 11(b), which, respectively, exhibit $\delta E_{\rm rms}$ for the same initial conditions as Figs. 9(c) and 9(d), now pulsed in c at frequencies $\Omega=10$ and 100. In these figures, the dotted curves represent the actual data, output at intervals $\delta t=5.0$., The solid curves, derived by boxcar averaging over, respectively, 10 and 20 time steps, exhibit the average value of $\delta E_{\rm rms}$, which, after the initial transient, is approximately constant. It is clear that, after the initial transient, the changes in energy, $\delta E_{\rm rms}$, computed for $\Omega=10$ and 100, do not exhibit the systematic diffusive behavior observed for $\Omega=1.0$. Rather, the value of $\delta E_{\rm rms}$ is approximately constant.

V. DISCUSSION AND IMPLICATIONS FOR GALACTIC DYNAMICS

Perhaps counter to naive expectations, chaotic orbits appear more susceptible overall to resonant driving than are regular orbits: Because regular orbits only have power at or near a few discrete frequencies ω_i, they must be driven with carefully chosen frequencies Ω to elicit a significant response. By contrast, because chaotic orbits have substantial power for a broader range of frequencies, it is much more likely that a randomly chosen Ω will be able to trigger a significant resonant coupling.

For a single chaotic orbit, the amplitude of the response to external driving is a very sensitive function of initial conditions, with a typical orbit executing an ap-

parent random walk in energy space. This explains the fact that, generically, the behavior exhibited by an ensemble of orbits will be intrinsically diffusive, with a Gaussian distribution of energy shifts, $N(\delta E(t))$, and an rms shift $\delta E_{\rm rms} \propto \alpha_{c,m} t^{1/2}$, where $\alpha_{c,m}$ denotes the amplitude of the periodic driving.

Several specific features of this phenomenon suggest that resonant driving of stochastic orbits could prove important for galactic potentials admitting global stochasticity. The most obvious fact is that the characteristic frequencies eliciting a significant response, namely, Ω between 0.05 and 5.0 or so, correspond to a characteristic time scale Ω^{-1} comparable to a dynamical, or crossing, time $t_{\rm cr}$. However, it is evident that time-dependent effects with such characteristic frequencies could arise naturally in response to either internal oscillations about some average, time-independent potential, or to the perturbing influences of some nearby galaxy.

Also significant is the fact that, for frequencies in this optimal range, even a relatively small amplitude driving can trigger a significant response within a time $t \sim 2000$, this corresponding to a Hubble time t_H. Consider, e.g., the case of stochastic orbit ensembles with initial energy $E = -0.5$, subjected to oscillations in c. Here, even a relatively tiny perturbation of fractional amplitude $\alpha_c = 10^{-3}$ suffices to induce an rms change in energy of approximately 6% within a time $t = 2000$; and, since the amplitude of the response scales linearly in α_c, increasing α_c to even slightly larger values implies significant fractional changes in a typical particle energy. However, such a characteristic amplitude is easily attributable to a relatively large nearby satellite, or companion, galaxy.

The response of an ensemble of stochastic orbits *does* manifest a relatively sensitive dependence on the specific value of the driving frequency. However, this dependence on Ω is much smoother than that exhibited by individual stochastic orbits. This is, e.g., illustrated in Fig. 12(a), which exhibits the value of $\delta E_{\rm rms}$ at $t = 1000$, generated for ensembles of stochastic orbits with $E = -0.5$, pulsed in c with fixed amplitude $\alpha_c = 10^{-4}$ but variable frequency Ω. Each frequency was sampled by at least one ensemble of 160 orbits and, in most cases, three ensembles were selected. The error bars reflect the dispersion for the computed values of $\delta E_{\rm rms}$. Figure 12(b) exhibits identical data for ensembles with $E = -0.3$. Overall, approximately 90% of the ensembles used to generate these figures exhibited a diffusive behavior with $\delta E_{\rm rms}$ growing as $t^{1/2}$, whereas the remaining 10% admitted various forms of "anomalous" behavior. The incidence of anomalous behavior was not significantly higher for frequencies where the response was particularly large (or small).

It is clear from Fig. 12 that, even in the natural frequency range, the amplitude of the response exhibits considerable variability but, for most values of the frequency, the response is, in fact, significant. This indicates again that a finely tuned frequency is not required to trigger a substantial response. In this regard, it should perhaps be observed that for $E = -0.5$, the frequency $\Omega = 1.0$, discussed in Sec. IV and used above to estimate the overall effects of periodic driving, actually corresponds to a relatively "bad" frequency, corresponding to a local minimum in $\delta E_{\rm rms}(\Omega)$.

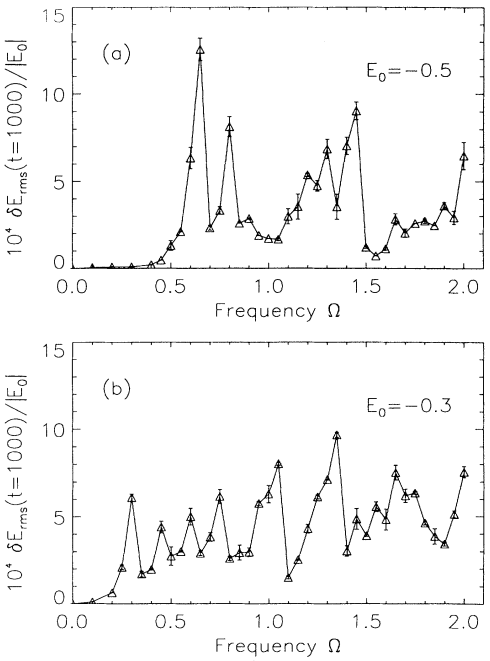

FIG. 12. (a) The rms change in energy $\delta E_{\rm rms}$ at $t = 1000$ computed for one or more ensembles of 160 unconfined stochastic orbits with $E = -0.5$, pulsed in c at amplitude $\alpha_c = 10^{-4}$ with variable frequency Ω. (b) The same for ensembles with $E = -0.3$.

Resonant driving could be important astronomically for a self-consistent near equilibrium because changes in the distribution of energies can induce changes in the bulk potential and, hence, alterations in the bulk distribution of matter, including the ejection of matter with positive energy. If the potential admits only regular orbits, resonant driving may be relatively unimportant, except at a few special frequencies, so that the system could perhaps readjust itself to minimize the effects of internal oscillations and/or an external environment. If, however, the self-consistent potential continues to evolve in such a fashion as to admit substantial global stochasticity, one might anticipate that resonant driving would persist as a nontrivial influence, triggering a continuing evolution.

ACKNOWLEDGMENTS

The authors acknowledge useful conversations with Salman Habib, M. Elaine Mahon, Randy Fisher, and John Papaloizou. Some of the simulations described herein were effected using time provided by the KSR Parallel Computing Research Laboratory at the University of Florida and by the Northeast Regional Data Center (Florida) by agreement with IBM Corp. H.E.K. was supported in part by the National Science Foundation through Grant No. PHY92-03333.

[1] Cf. M. Hénon and C. Heiles, Astron. J. **69**, 73 (1964); G. Contopoulos, Astron. J. **76**, 147 (1971); G. Contopoulos and B. Barbanis, Astron. Astrophys. **222**, 329 (1989); D. E. Kaufmann, Ann. N.Y. Acad. Sci. (to be published), and references cited therein.
[2] J. N. Mather, Topology **21**, 45 (1982).
[3] H. E. Kandrup and M. E. Mahnon, Astron. Astrophys. **290**, 762 (1994).
[4] M. E. Mahon, R. A. Abernathy, B. O. Bradley, and H. E. Kandrup, Mon. Not. R. Astron. Soc. (to be published).
[5] A. Toomre and J. Toomre, Astrophys. J. **178**, 623 (1972).
[6] F. Schweizer, Science **231**, 227 (1986); C. Norman, in *IAU Colloquium 124—Paired and Interacting Galaxies,* edited by J. W. Sulentic, W. C. Keel, and C. Telesco, NASA Conference Publication No. 2098 (NASA, Washington, D.C., 1990), p. 765.
[7] S. E. Zepf and B. C. Whitmore, Astrophys. J. **418**, 72 (1993).
[8] S. Udry and D. Pfenninger, Astron. Astrophys. **198**, 135 (1988).
[9] H. Hasan and C. Norman, Astrophys. J. **361**, 69 (1990).
[10] S. Sridhar, Mon. Not. R. Astron. Soc. **238**, 1159 (1989).
[11] P. Mineau, M. R. Feix, and J. L. Rouet, Astron. Astrophys. **228**, 344 (1990).
[12] R. H. Miller and B. F. Smith, Celestial Mechanics **59**, 161 (1994).
[13] D. Armbruster, J. Guckenheimer, and S. Kim, Phys. Lett. A **140**, 416 (1989).
[14] Cf. R. Z. Sagdeev, D. A. Usikov, and G. M. Zaslavsky, *Nonlinear Physics: From the Pendulum to Turbulence and Chaos* (Harwood, New York, 1988), as applied to galactic dynamics by J. J. Binney and D. Spergel, Astrophys. J. **252**, 358 (1982); Mon. Not. R. Astron. Soc. **206**, 159 (1984).
[15] Cf. J.-P. Eckmann and D. Ruelle, Rev. Mod. Phys. **57**, 617 (1985).
[16] H. E. Kandrup, R. A. Abernathy, M. E. Mahon, and B. O. Bradley, Ann. N.Y. Acad. Sci. (to be published).
[17] A. J. Lichtenberg and M. A. Lieberman, *Regular and Chaotic Dynamics* (Springer-Verlag, Berlin, 1992).